Theoretical Studies on the Mechanism of Conversion of Androgens to Estrogens by Aromatase†

Kenneth R. Korzekwa,* William F. Trager,‡ Soozy J. Smith,§ Yoichi Osawa,§ and James R. Gillette§
Laboratory of Chemical Pharmacology, National Heart, Lung, and Blood Institute, National Institutes of Health, Bethesda, Maryland 20892, and Department of Medicinal Chemistry, University of Washington, Seattle, Washington 98195
Received August 17, 1990; Revised Manuscript Received March 28, 1991

ABSTRACT: Semiempirical molecular orbital calculations (AM1) were used to model several possible reaction mechanisms for the third oxidation of the aromatase-catalyzed conversion of androgens to estrogens. The reaction mechanisms considered are based on the assumption that the third oxidation is initiated by 1β-hydrogen atom abstraction. Homolytic cleavage of the C_{10}–C_{19} bond was modeled for both the 3-keto and 2-en-3-ol forms of the androgen 1-radicals. The addition of a protein nucleophile to the 19-oxo intermediate was also considered, and $-OCH_3$, $-SCH_3$, and $-NHCH_3$ were used to represent the Ser, Cys, and Lys adducts. The transition states were estimated and optimized from the reaction coordinates obtained by constraining and increasing the C_{10}–C_{19} bond lengths. The enthalpies of activation range from 14 to 21 kcal and are ~2 kcal lower for cleavage of the enol form. Given the tendency for AM1 to overestimate activation energies, all reactions may be energetically accessible. Other reactions modeled include a homolytic cleavage reaction from a thioether radical cation and the direct additions of oxygen radical compounds to the carbonyl of the 1-radical-2-en-3-ol-19-oxo androgen. A mechanism is proposed in which the 19-oxo intermediate is subject to initial nucleophilic attack by the protein. Since rotation of the 19-carbonyl can bring the oxygen within 2.1 Å of the 2β-hydrogen, the formation of a tetrahedral intermediate can occur with concomitant removal of the 2β-proton. Enolization activates the C_1-position for hydrogen atom abstraction, since the resulting radical is resonance stabilized. Homolytic cleavage of this radical is followed by recombination of the C_{19}-radical with the hydroxy radical equivalent. The geometry of the carbonyl oxygen in the androgens is between that for the 1-radicals and estrogen, suggesting that some transition-state stabilization for the homolytic cleavage reaction may occur.

The cytochrome P-450 enzymes are a superfamily of monooxygenases capable of oxidizing a wide variety of both exogenous and endogenous compounds (Ortiz de Montellano, 1987; Guengerich, 1987). Where as many of the isozymes have broad substrate specificity and have apparently evolved for the metabolism of foreign compounds, some of the isozymes are very specific for certain endogenous substrates. One of the most remarkable cytochrome P-450s is aromatase, the enzyme responsible for the conversion of androgens to estrogens. This enzyme has received considerable attention over the last 30 years (Ryan, 1959; Engle, 1973), with much of the effort directed at the development of inhibitors to be used in the treatment of estrogen-dependent breast cancer (Brodie et al., 1982; Santen, 1982; Siteri, 1982; Van Wauwe & Janssen, 1989).

The general reaction sequence for aromatase is shown in Scheme I. It has been shown that three molecules of molecular oxygen and six reducing equivalents from NADPH are consumed during estrogen formation (Thompson & Siiteri, 1974). The androgen is first oxidized to the C_{19}-hydroxy androgen and then oxidized to the C_{19}-*gem*-diol or its dehydrated form, the C_{19}-aldehyde. The mechanism of the third oxidation is still undefined, even though considerable information regarding the reaction has been established over the years. For example, it is known that the specific removal of both the 1β- and 2β-hydrogens (Townsley & Brodie, 1968; Brodie et al., 1959; Fishman et al., 1969; Osawa & Spaeth, 1971) and the incorporation of an atom from molecular oxygen into formate (Akhtar et al., 1981; Stevenson et al., 1985), the final form of the C_{19}-methyl group, are obligatory steps in the reaction sequence. Most of the proposed detailed mechanisms for this step have been precluded by these requirements. The requirements are still consistent with a mechanism that has received attention in recent years that postulates the addition of the ferric peroxy anion from aromatase to the C_{19}-aldehyde. The resulting alkyl peroxy intermediate then decomposes either in a direct manner (Cole & Robinson, 1988) or via the 10-hydroxy intermediate (Watanabe & Ishimura, 1989a,b) to give the estrogen as the final product. In support of this mechanism is the demonstration that the protected enol of the 19-oxo androgen is converted to the estrogen upon treatment with hydrogen peroxide (Cole & Robinson, 1988). Although the involvement of a 10-hydroxy intermediate has been shown to be unlikely (Covey et al., 1984; Caspi et al., 1989), a peroxide-mediated mechanism is consistent with the available data. However, some aspects of this mechanism remain troubling. For example, a wealth of evidence suggests that the catalytically competent species generated by cytochrome P-450 is a ferric-bound oxygen atom (oxene). Indeed, this species is believed to mediate the first two oxidative steps in the aromatase reaction. If this is true, then the requirement of a totally different form of activated oxygen for the third step seems puzzling. So far as we are aware, documentation of a cytochrome P-450 catalyzed addition of peroxy anion to a carbonyl group has not appeared in the literature. This question then arises: Is aromatase unique, or are other mechanisms possible that involve an oxene as the reactive oxygen species and that are equally or more consistent with

† Supported in part by the National Institutes of Health (Grant GM 36922) and in part by a PRAT Fellowship (K.R.K.) from the National Institutes of General Medical Sciences.
* To whom correspondence should be addressed at Laboratory of Molecular Carcinogenesis, National Cancer Institute, National Institutes of Health, Building 37, Room 3E24, Bethesda, MD 20892.
‡ University of Washington.
§ National Heart, Lung, and Blood Institute.

0006-2960/91/0430-6155$02.50/0

Scheme I

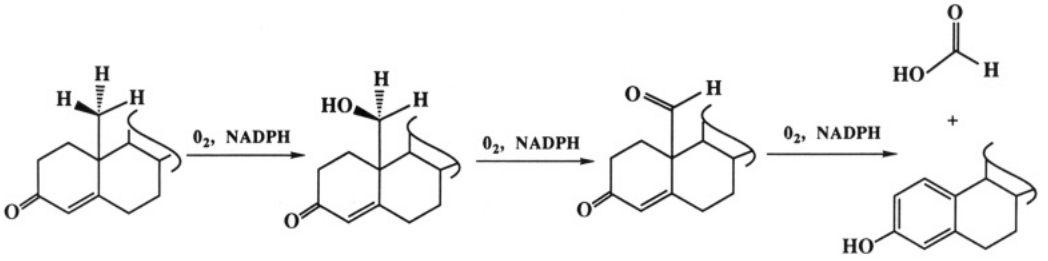

Scheme II

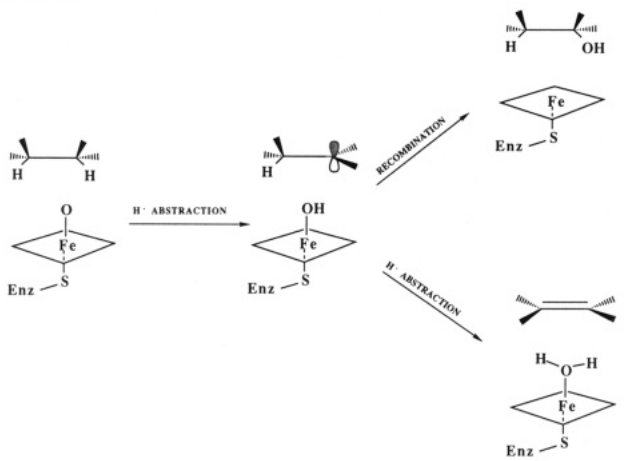

the available experimental data?

Covey and co-workers (Beusen et al., 1987; Covey et al., 1987) have discussed a general oxene mechanism in which 1β-hydrogen abstraction precedes homolytic cleavage of the C_{10}–C_{19} bond. Two observations provide support for a modified version of this mechanism. (1) Consideration of molecular models indicated that the carbonyl oxygen of the C_{19}-aldehyde can approach the 2β-hydrogen to within 2.1 Å. Promotion of the removal of the 2β-hydrogen by the C_{19}-carbonyl would account for the experimentally known stereospecific loss of this hydrogen atom as well as the catalyzing enolization of the 3-keto group, which is mandatory for product formation. (2) Mechanistic studies on the cytochrome P-450 catalyzed desaturation reactions (Scheme II) suggest that the hydroxy radical equivalent formed by hydrogen atom abstraction is not always committed to recombination with the radical (Nagata et al., 1986; Rettie et al., 1987, 1988; Korzekwa et al., 1990a). With regard to the first observation, the C_{19}-carbonyl could efficiently effect enolization by undergoing an initial attack by a nucleophile from an appropriate amino acid residue of the apoprotein. Presumably, this amino acid would be part of the construct of the active site of the enzyme and would be critically oriented for catalysis. Such an attack would generate an oxygen anion whose carbon–oxygen bond would be elongated relative to the carbon–oxygen double bond, bringing the negative charge in even closer proximity to the 2β-hydrogen and thereby catalyzing enolization. After enolization has occurred, the energy of activation for removal of the 1β-hydrogen by cytochrome P-450 to generate a carbon-based radical at C_1 would be lowered by resonance stabilization. This analysis together with the second observation led us to speculate that abstraction of the 1β-hydrogen atom might precede C_{10}–C_{19} bond cleavage and occur with minimal recombination to the hydroxy radical. Osawa et al. (1987a,b) found that substantial amounts of 1β- and 2β-hydroxy androgens are formed by aromatase when the C_{19}-methyl group is completely tritiated, suggesting that both sites (1β and 2β) are accessible to the active oxygen and susceptible to attack when the conditions are appropriate. The next step in the postulated mechanism would be the aromatization of the A-ring of the steroid by homolytic cleavage of the C_{10}–C_{19} bond. This would then be followed by addition of the hydroxy radical equivalent to the C_{19}-radical to generate an orthoformate-bound enzyme and estrogen (Scheme III).

In order to evaluate possible oxene-based mechanisms for the third oxidative step in the aromatase reaction, semiempirical theoretical calculations (AM1) were used to model various hypothetical reaction pathways. The results of these calculations are the subject of this paper.

Methods

The semiempirical quantum chemical calculations were performed on a Microvax II with use of the AM1 (Dewar et

Scheme III

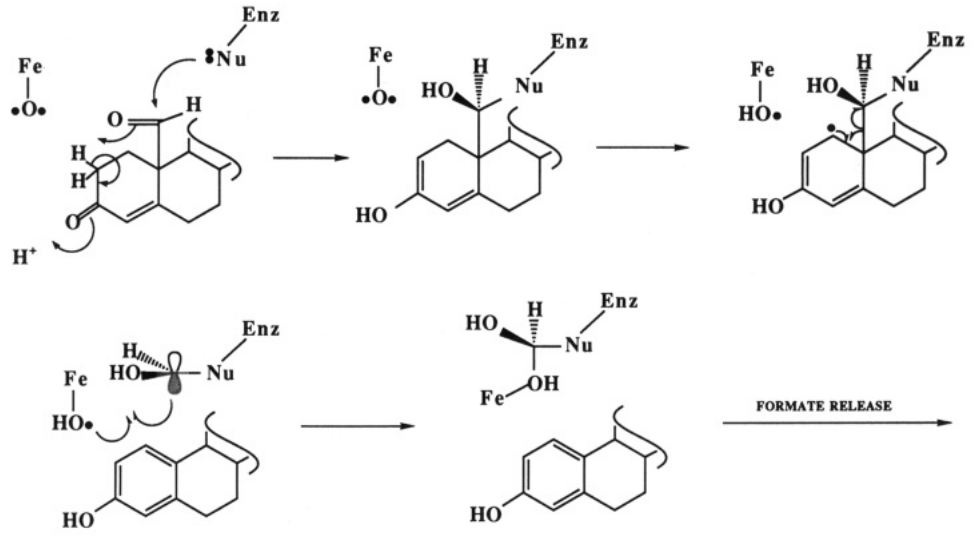

Scheme IV

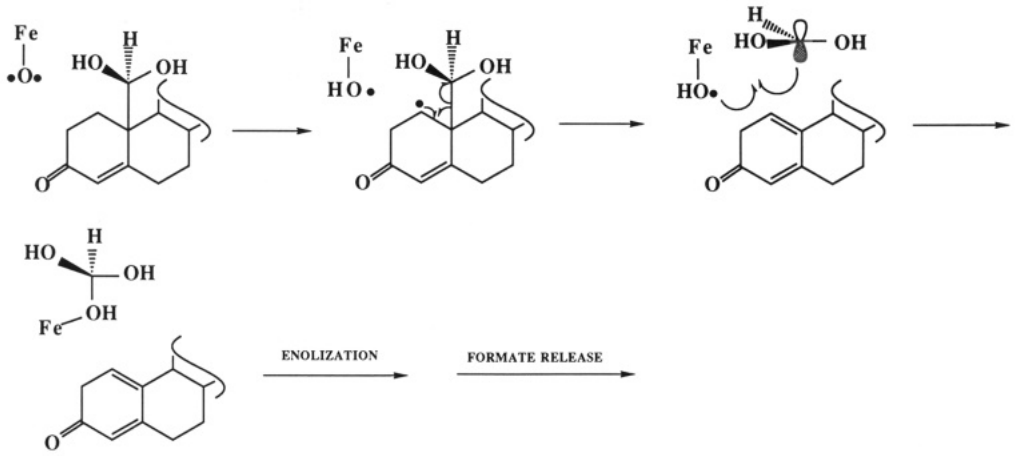

al., 1985) formalism as found in MOPAC 5.0 (QCPE 455), modified to include the parameters for sulfur given in AMPAC 2.1. The UHF Hamiltonian was used for all open-shell calculations. Stable geometries were optimized from approximate starting geometries, and reaction coordinates were generated by constraining and varying the appropriate oxygen–carbon or carbon–carbon bond lengths. Approximate transition states were optimized with the gradient minimization routines provided by MOPAC. SCF calculations were optimized to $<10^{-8}$ kcal/mol, and geometries were optimized to $<10^{-4}$ Å. All stable geometries and transition states were verified by the presence of 0 and 1 negative eigenvalues of the force constant matrix, respectively.

Results

Relative Stabilities of the Ketones, Enols, and Their C_1-Radicals. In order to determine the influence of the C- and D-rings on the reactions, the initial compounds were modeled by utilizing the complete steroid nucleus (testosterone) and the simplified AB-ring analogues. As discussed by Covey et al. (1987), enolization of the 2-position could occur either before the formation of the C_1-radical between C_1-radical formation and bond cleavage or after C_{10}–C_{19} bond cleavage. The calculated enthalpies of formation for testosterone (and AB-ring analogue), their 2-en-3-ols, and the C_1-radicals of these compounds are given in Figure 1. As expected, the calculated heats of reaction for enolization show that the keto–enol equilibrium for testosterone greatly favors the keto form. The calculated stabilities of the C_1-radicals relative to their parent compounds show that the relative stability of the testosterone C_1-radical (28.4 kcal/mol) is similar to that for other secondary-carbon radicals (cyclohexane = 28.6, propane = 27.7, decalin = 28.6–29.0; data not shown). In contrast, the C_1-radical of the 2-en-3-ol (9.8 kcal/mol) is substantially more stable. Finally, the results in Figure 1 ($H_{R(enol)}$ and radical stability) show that the C- and D-rings of the steroids do not substantially affect the electronic properties of the A- and B-rings. Therefore, all subsequent calculations were done on the AB-ring analogues.

Homolytic Cleavage of 19-Substituted Analogues from the 1-Radicals. In the mechanism initially proposed by Beusen, Carrell, and Covey (1987), cleavage of the C_{10}–C_{19} bond occurs after abstraction of the 1β-hydrogen atom from the 19-diol (Scheme IV). We have modeled this reaction as well as a similar reaction from the 2-en-3-ol (Scheme III). We have considered the possibility that the 19-diol dehydrates to form the aldehyde, which is then subject to attack from a protein nucleophile. Therefore, in addition to the 19-diol, we have included the analogues that contain both –OH and

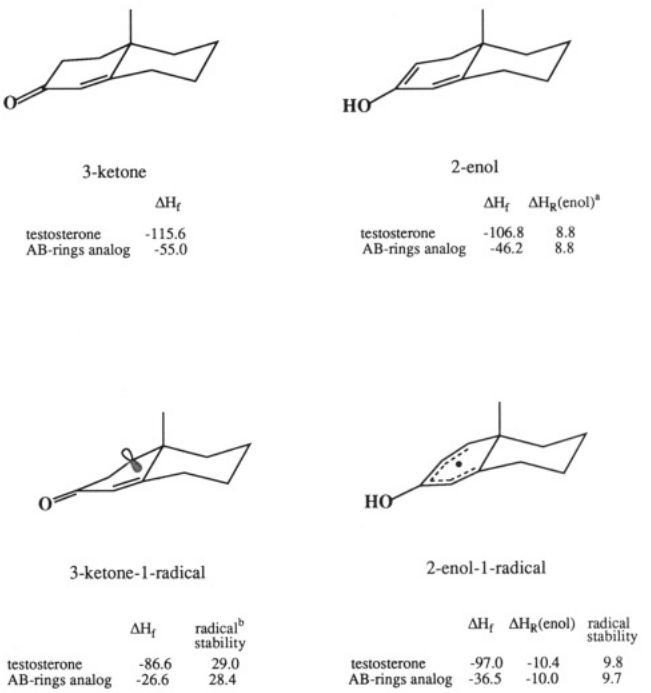

3-ketone

	ΔH_f
testosterone	-115.6
AB-rings analog	-55.0

2-enol

	ΔH_f	$\Delta H_R(enol)^a$
testosterone	-106.8	8.8
AB-rings analog	-46.2	8.8

3-ketone-1-radical

	ΔH_f	radical[b] stability
testosterone	-86.6	29.0
AB-rings analog	-26.6	28.4

2-enol-1-radical

	ΔH_f	$\Delta H_R(enol)$	radical stability
testosterone	-97.0	-10.4	9.8
AB-rings analog	-36.5	-10.0	9.7

FIGURE 1: Calculated heats of formation (AM1) and heats of reaction for testosterone and its AB-ring analogue: [a]heat for reaction enolization; [b]heat of formation of the radical – heat of formation of the parent compound.

Homolytic cleavage of 3-keto-1-radicals

	$\Delta H_f(rad)^a$	$\Delta H_f(TS)^b$	$\Delta H^\dagger$
R = OH	-123.8	-103.8	20.0
R = SCH_3	-63.2	-42.3	20.9

Homolytic cleavage of 2-enol-1-radicals

	ΔH_f(sub)	ΔH_f(TS)	$\Delta H^\dagger$
R = OH	-134.1	-116.0	18.1
R = SCH_3	-73.8	-55.0	18.8
R = OCH_3	-128.5	-108.5	20.0
R = NCH_3(S)	-74.9	-58.3	16.6
R = NCH_3(R)	-72.0	-58.0	14.0

FIGURE 2: Calculated thermodynamic properties (AM1) for C_{10}–C_{19} homolytic cleavage reactions: [a]heat of formation of the radical; [b]heat of formation of the transition state.

–$NHCH_3$, –OCH_3, or –SCH_3 at the 19-position (representing lysine, serine or threonine, or cysteine addition to the aldehyde; Scheme III). In all cases, homolytic cleavage was achieved by constraining and increasing the C_{10}–C_{19} bond length. The thermodynamic properties of the reactants, transition states,

Scheme V

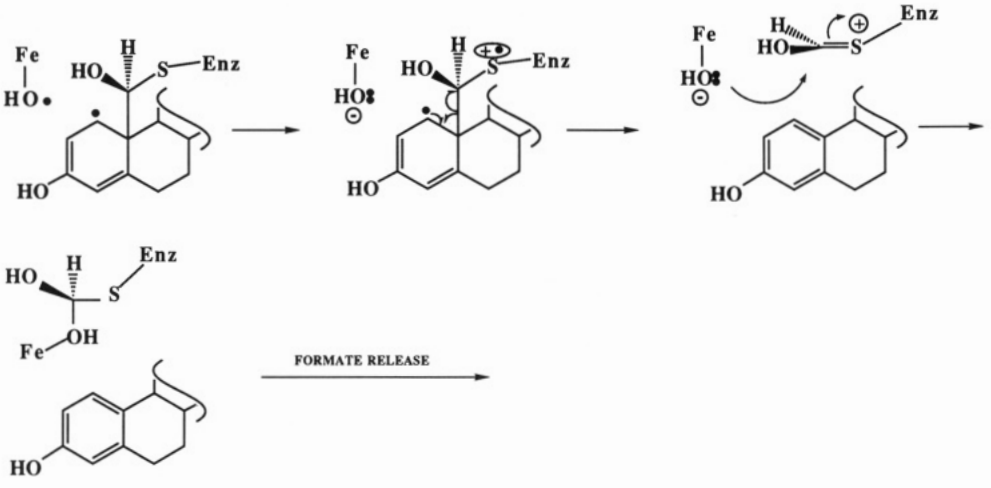

Scheme VI

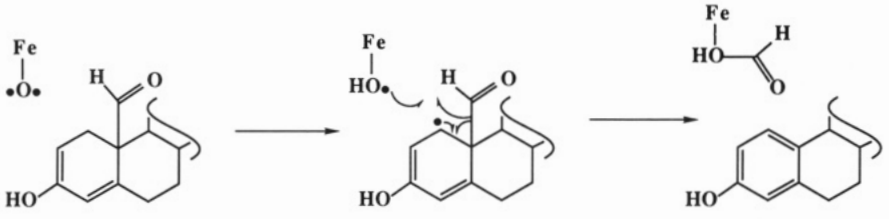

and products are given in Figure 2. The enthalpies of activation ranged from 14.0 kcal/mol for R = $-NHCH_3$ to 20.0 kcal/mol for R = $-OCH_3$. For R = –OH and R = $-SCH_3$, the enthalpies of activation for homolytic cleavage of the enol forms of the radicals are about 2 kcal/mol lower in energy than those for the corresponding keto forms. Also, similar differences in activation enthalpies for these two substitutions within each reaction suggest that stabilization characteristics for the two reactions are similar.

Homolytic Cleavage of Sulfur Radical Cation Analogues. In addition, we have considered the possibility that after cysteine adduct formation an electron is abstracted from the sulfur atom after abstraction of the 1-hydrogen atom to aid in homolytic cleavage (Scheme V). Such electron abstraction reactions have been proposed as the first step in other cytochrome P-450 mediated oxidations (Ortiz de Montellano, 1989). Since the hydroxyl radical equivalent formed by hydrogen atom abstraction is apparently capable of abstracting an additional hydrogen atom (Korzekwa et al., 1990a), the abstraction of an electron to form a hydroxide intermediate seems plausible. In order to model this reaction, a biradical cation species is required, with one unpaired electron in the A-ring of the steroid and one unpaired electron on the sulfur. Since the lowest energy cation for the thiomethyl adduct of the 2-en-3-ol form will have the cation in the A-ring (closed-shell cation), it was necessary to generate the required electronic configuration (biradical cation) by abstracting an electron from the sulfur atom with a proton. This was accomplished by first protonating the sulfur atom and then generating a reaction coordinate where the hydrogen–sulfur distance is slowly increased to 30 Å, beginning the SCF calculation at each point with the density matrix from the previous point. Unfortunately, while the biradical cation could be generated in this manner, when the C_{10}–C_{19} bond length was increased to induce homolytic cleavage, the thiomethyl cation rotated above and formed a bond to the C_1-position. In order to prevent this interaction, the thiomethyl position was constrained by attaching the methyl carbon to the $C_8\beta$-position of the B-ring (Figure 3). It was then necessary to compare a homolytic cleavage reaction with the constrained structure to the same reaction for the unconstrained structure. Cleavage of the C_{10}–C_{19} bond for the 1-radical-2-en-3-ol thiomethylene compound gave an enthalpy of activation of 17.4 kcal/mol, 1.4 kcal lower than that for the unconstrained thiomethyl analogue. This lower activation enthalpy is due to conformational strain associated with attaching the thiomethyl group to the C_8-position, some of which is relieved in the transition state. A proton was then used to abstract an electron from the sulfur giving the constrained biradical cation. Homolytic cleavage of this compound had an activation energy of 17.0 kcal/mol, 0.4 kcal/mol lower than that for the noncation.

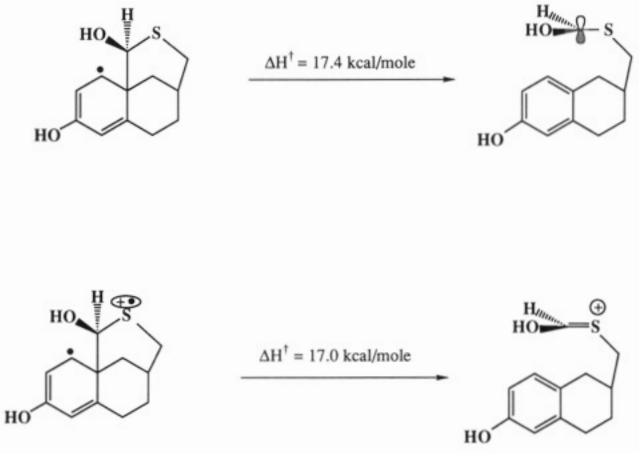

FIGURE 3: Activation enthalpies for C_{10}–C_{19} cleavage of the constrained radical and biradical cations.

Addition of Various Oxygen Radicals to the 1-Radical-2-en-3-ol-19-oxo Steroid Analogue. In a manner analogous to that proposed for cytochrome P-450 mediated desaturation reactions, a simple reaction mechanism involving the addition of various oxygen-radical species to the carbonyl carbon of the 1-radical-2-en-3-ol-19-oxo steroid analogue was modeled

(Scheme VI). Addition of a hydroxy radical to the 19-carbonyl on the UHF surface resulted in a smooth reaction coordinate from reactants to products (formate and the estrogen analogue). A transition state for the reaction was characterized and had an activation energy of 9.6 kcal/mol. While this activation energy is quite low, particularly for AM1/MNDO calculations, the tremendous reactivity of the hydroxy radical (and the associated exothermicity of the reaction) suggests that this radical is not appropriate to model cytochrome P-450 mediated reactions (Korzekwa et al., 1990b). However, when more stabilized radicals were used, in particular the phenoxy and ethyleneoxy radicals, a "chemical hysteresis" resulted (Friedrich et al., 1988), with a sudden change in electronic structure occurring before a transition state was reached. Although the addition of the phenoxy radical proceeded smoothly to the point where the reaction coordinate gradient began to decrease, the transfer of the radical from the aromatic ring to the carbonyl oxygen resulted in a sudden decrease in energy. Further addition resulted in a tetrahedral intermediate, which had a small barrier for cleavage of the C_{10}–C_{19} bond to give products. Beginning with the tetrahedral intermediate and increasing the C_{19}–O bond length resulted in similar behavior, with the reaction proceeding with the radical on the carbonyl oxygen and then changing to the electronic structure with the radical in the aromatic ring. However, observation of the energy relative to the reaction gradients suggests that the activation energies associated with the transition states on both potential energy surfaces exceed 30 kcal/mol.

Discussion

The intent of this study was to explore the energetics for mechanisms leading to the aromatization of the 19-oxo androgens that rely on the oxene species of cytochrome P-450 and that are consistent with presently available experimental data. The general mechanisms that have been considered have been discussed previously by Covey et al. (1987) and involve abstraction of the 1β-hydrogen atom by the oxene prior to cleavage of the C_{10}–C_{19} bond. While this abstraction can occur from either the 3-keto or 2-en-3-ol androgens, abstraction from the enol form offers two advantages over abstraction from the keto form. First, the 1-radical would be conjugated to the adjacent 2,4-dien-3-one, lowering the activation energy for the reaction. The AM1 results in Figure 1 show that the conjugated radical is 19 kcal/mol more stable than the unconjugated radical. A recent study using a model oxygen radical to predict the tendency for hydrogens to be abstracted by cytochrome P-450 (Korzekwa et al., 1990b) suggests that the activation energy should be lowered by 30%.[1] In addition to activating the 1-position, the stability of the radical would also increase the activation energy for recombination, allowing alternative reactions to take place.

In the mechanism proposed in Scheme III, the C_{19}-carbonyl is subject to initial attack by a nucleophilic residue provided by the apoprotein with concomitant removal of the 2β-proton to generate the enol. Since the hypothetical nucleophilic amino acid is unknown, calculations were performed on various likely possibilities. Thus, the C_{19}-carbonyl addition products containing –OH, $-OCH_3$, $-NHCH_3$, and $-SCH_3$ were selected to mimic the addition of H_2O, serine, lysine, and cysteine. In addition, the pathway involving homolytic cleavage of the C_{10}–C_{19} bond from the 3-keto-1-radical to the C_{19}-*gem*-diol has been modeled to provide an energy estimate for the mechanism proposed by Beusen et al. (1987). This reaction was also modeled with the $-SCH_3$ addition product in order to compare the two reactions.

For homolytic cleavage reactions from the 2-enol forms of the 1-radicals, the enthalpies of activation for the serine and cysteine models were found to be 20.0 and 18.8 kcal/mol, respectively (Figure 2). Two different conformations with respect to the nitrogen lone pair of the enol methylamine addition product gave activation enthalpies of 16.6 kcal/mol for the (*S*)-amine conformation and 14.0 kcal/mol for the (*R*)-amine conformation. The lower value of the (*R*)-conformation appears to be due to steric interactions of the amine proton with the B-ring in the ground state. The starting geometries used in all calculations were chosen to be the local minima corresponding to attack of the protein nucleophile from the C_{11}-direction.

The range of energies found (14.0–20.0 kcal/mol) is not sufficient to preclude the involvement of any one of the amino acids considered as the nucleophilic species. Moreover, the tendency for MNDO (AM1) to overestimate activation energies suggests that the involvement of an amino acid nucleophile in the reaction sequence is energetically feasible. Thus, given the favorable energetics for the formation of the C_1-radical after enolization and the possibility of catalyzing enolization by nucleophilic attack, invoking the formation of the enolic 1-radical prior to C_{10}–C_{19} bond cleavage appears justified. Nevertheless, the relative energetics for C_{10}–C_{19} bond cleavage without prior enolization, that is, from the ketone, should be considered and compared to the energetics for C_{10}–C_{19} bond cleavage after enolization.

Homolytic cleavage of the C_{10}–C_{19} bond after 1β-hydrogen abstraction was first proposed by Beusen et al. (1987). In this mechanism, we propose that abstraction and cleavage occurs from the 1-radical-3-keto-19-*gem*-diol intermediate (Scheme IV). The hydroxy radical then recombines with the *gem*-diol radical to form orthoformate. Enolization occurs when orthoformate deprotonates the 2β-position during dehydration to give the estrogen and formate. Provided that the oxygen atom from the second oxidation abstracts the 2-proton and is lost as water, this mechanism accounts for loss of the 1β- and 2β-protons as well as the incorporation of the first and third oxygen atoms into formate.

Homolytic cleavage reactions for the *gem*-diol and the methanethiol addition product were modeled for both the ketone and enol form. For both compounds, the enthalpies of activation for the enol forms were ~2 kcal/mol lower than for the keto forms (Figure 2).

Thus, the major difference between the protein adduct mechanism proposed here and that of Beusen et al. (1987) resides clearly not in the energetics for C_{10}–C_{19} bond cleavage from the C_1-radicals but instead in the difference in energy required for C_1-radical formation.

Two additional mechanisms that were considered include homolytic cleavage of the C_{10}–C_{19} bond from the thio radical cation addition product and the direct addition of hydroxy radical to the 19-carbonyl group. Although the transition state for cleavage of the C_{10}–C_{19} bond from the radical cation was slightly lower (0.4 kcal/mol) than that for the corresponding thio species, such a small difference in energy does not justify

[1] The activation energy for this reaction was predicted from calculated radical stabilities and ionization potentials of the 3-keto and 2-enol AB-ring analogues as in Korzekwa et al. (1990b). The calculated activation energies are given in Figure 5. Since the computational methods tend to overestimate activation energies, the results should be considered qualitative. Since the predictive method was normalized by transition-state symmetry, discussions of fractional changes in activation energies may be more valid.

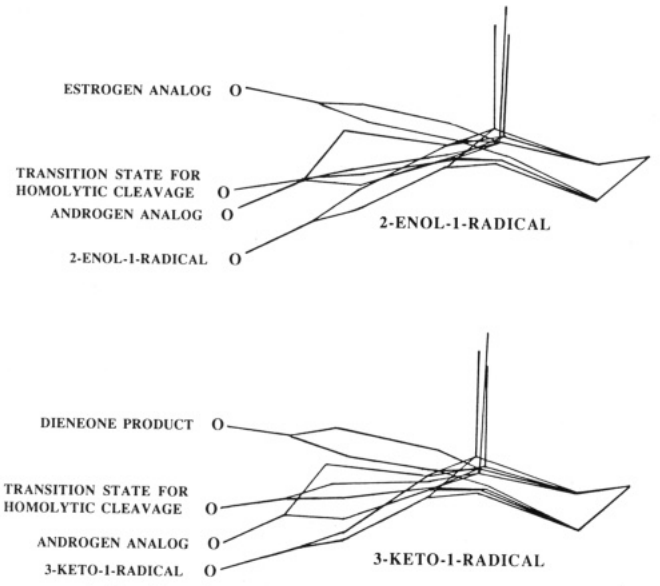

FIGURE 4: Overlay of geometries for 2-enol and 3-keto forms of the substrates, intermediates, transition states, and products.

invoking an additional electron abstraction step.

The gas-phase calculation for the addition of a hydroxy radical to the 1-radical-2-en-3-ol (Scheme VI) proceeds smoothly with concomitant homolytic cleavage to give the aromatic product and formate with $\Delta H = 9.6$ kcal/mol. The activation energy for the addition of a hydroxy radical is probably much lower than would be calculated for a heme-stabilized hydroxy radical. Although transition states could not be obtained for addition of the more stable phenoxy and ethyleneoxy radicals, the estimated activation energies were > 30 kcal/mol. However, although the activation energy for direct addition of a more stabilized hydroxy radical species (as is expected to be delivered by the enzyme) would be higher than that for the hydroxy radical, the direct-addition mechanism remains a possibility, since the transition-state symmetry for the recombination reaction and, therefore, the characteristics of the hydroxy radical equivalent remain unknown.

An additional advantage for homolytic cleavage after initial 1β-hydrogen abstraction can be seen if the geometries of the compounds are considered. Table I gives the C_9–C_8–C_7–C_x dihedral angles for the full steroids modeled and a representative group of partial steroids. The similarities between the complete steroids and their AB-ring analogues suggest that alignment of the C_7, C_8, and C_9 atoms will provide a reasonable model for comparing potential protein steroid interactions. Both the enol and ketone form of the 1-radical have geometries with the A-ring bent below the plane of the steroid (similar

Table I: Dihedral Angles (C_9–C_8–C_7–C_x) for Selected Optimized Geometries and Transition States

	τ					
compound	$x = 6$	$x = 5$	$x = 4$	$x = 3$	$x = 2$	$x = 1$
testosterone (T)	301.6	328.1	333.9	338.8	337.7	344.7
T A-analogue (TAB)	303.3	329.1	334.7	339.6	339.1	346.3
T 2-enol	301.0	327.4	331.9	337.0	341.2	345.0
TAB 2-enol	301.2	327.7	331.9	337.1	341.6	345.8
T 2-enol-1-radical	303.2	330.3	339.2	345.3	346.6	343.1
TAB 2-enol-1-radical	305.0	331.9	339.9	346.1	348.3	345.3
TAB 1-radical	304.4	330.9	338.2	343.8	344.7	345.3
estrogen AB-analogue	298.3	321.5	319.1	325.3	339.1	346.3
TS 2-enol-1-radical	301.2	327.4	329.5	336.4	342.6	345.0
TS 3-keto-1-radical	300.3	326.6	328.5	335.3	340.7	344.5

to the geometry reported for androsta-1,4-dien-3-one steroids; Duax, 1971) while the product estrogen has an A-ring that is bent up above the steroid (see Figure 4, top and bottom). The large change in the geometry of the product has been postulated to cause a fast rate of product release (Osawa, 1973). Both the androgens and the transition states for homolytic cleavage have A-ring geometries that are between reactants (1-radicals) and products (estrogens). If polar interactions between the 3-carbonyl (or enol) and the enzyme are involved in binding, the transition state for the enol may be bound more tightly than that for the ketone, since the position of the oxygen atom is closer to that for the androgen substrate. The K_m for androstenedione is 10 nM, which corresponds to a large amount of binding energy (11.3 kcal/mol, provided K_m approximates K_b). This suggests that substantial transition-state stabilization may be involved in the homolytic cleavage reaction. These binding influences will be limited to the cleavage reaction, since enolization (Table I) and substitution at C_{19} do not result in large changes in geometry.

The mechanisms of suicide inhibitors for aromatase can also be used to evaluate the reaction pathways proposed above. The presence of a nucleophile in the active site of aromatase is strongly suggested by time-dependent irreversible inactivation caused by the 19,19-difluoroandrost-4-ene-3,17-dione (Marcotte & Robinson, 1982). This compound is presumably metabolized to the acylfluoride that covalently binds to an active site nucleophile. It has also been shown that 6β-bromoandrostenedione but not 6α-bromoandrostenedione is a mechanism-based irreversible inhibitor of aromatase (Osawa et al., 1987c). From the enol form of the 1-radical, homolytic cleavage of the C_6–Br bond could compete with C_{10}–C_{19} bond cleavage, giving the 1,3,5-trien-3-ol, a bromine radical, and a hydroxy radical equivalent. Addition of the hydroxy radical to the unsaturated steroid would result in a carbon-based radical. Carbon-based radicals have been known to cause both

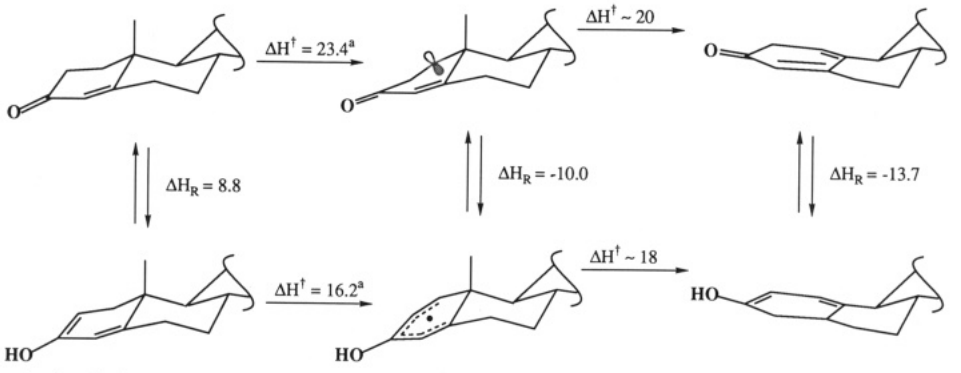

FIGURE 5: Overall calculated thermodynamic properties (AM1) for potential pathway for the aromatization of androgens. [a]Calculated as in Korzekwa et al. (1990b).

heme modification and cross-linking of the heme to the apoprotein (Osawa et al., 1990, 1991). Since the 6β-position is axial, this reaction is possible for the 6β-bromo analogue but not for the 6α-bromo analogue. If this mechanism is correct, it suggests that C_{10}–C_{19} bond cleavage occurs from the 2-en-3-ol form of the 1-radical.

A general scheme showing the relative thermodynamic properties of both the 3-keto and 2-en-3-ol androgens is shown in Figure 5. On the basis of this information and the above discussion, we favor the following mechanism. The active oxygenating species is situated closest to the C_{19}-methyl group and above the C_1- and C_2-carbon atoms (Kellis et al., 1987; Osawa et al., 1987a,b). The substrate remains in the keto form for the first two oxidations, which occur at the C_{19}-methyl group to give the 19-oxo intermediate. Addition of an active site nucleophile to the aldehyde catalyzes the enolization of the 2-position, activating the C_1-position. Abstraction of the 1β-hydrogen atom gives a radical intermediate with a decreased binding energy due to large geometry changes in the A-ring of the steroid. The binding energy is then regained at the transition state, lowering the energy of activation. The hydroxy radical equivalent recombines with the substituted methyl radical to give an orthoformate analogue from which formate is released. The above mechanism accounts for the selective loss of the 1β- and 2β-hydrogen atoms and the incorporation of the third atom from molecular oxygen into formate.

The position of the active oxygen relative to the substrate is supported both by the small amount (~1% each) of 1β- and 2β-hydroxylation (Osawa et al., 1987a,b)] and by the stereoselective binding of type II inhibitors (Kellis et al., 1987). The advantage of an aldehyde-induced enolization reaction is that the 1-position will be deactivated until the third oxidation. If the ratio of 19-hydroxylation to 1β- and 2β-hydroxylations is due to substrate orientation (binding interactions), this would correspond to an energy difference of ~3 kcal/mol. The predicted decrease in activation energy for 1β-hydrogen atom abstraction due to conjugation with the dienol is 7 kcal/mol.[1] While this prediction should be considered qualitative, even 1 kcal/mol would result in a substantial amount of 1β-hydroxy androgen. Although it is possible that the 1% 1β-hydroxylation is due to a small amount of enol in equilibrium with the keto form, it would require that the 1β and 2β-products be formed from different species, since 2β-hydroxylation cannot occur from the 2-enol. Osawa et al. (1987a,b) have shown that for [19-$^3H_3$]androstenedione both 1β- and 2β-hydroxylation are greatly increased. Therefore, both 1β- and 2β-hydroxylation reactions are in direct competition with 19-hydroxylation. In addition, although the calculated activation enthalpies for homolytic cleavage reactions are only 10% lower for the enol forms, the rate of radical recombination (which would be in competition with C_{10}–C_{19} cleavage) should be substantially faster for the isolated σ-radical of the 3-ketone than for the conjugated π-radical of the 2-enol. Finally, the calculated transition states for homolytic cleavage of both the ketones and enols have geometries similar that of to the initial androgen, suggesting that the substrate binding characteristics are also involved in transition-state stabilization.

References

Akhtar, M., Calder, M. R., Corina, D. L., & Wright, J. N. (1981) *J. Chem. Soc., Chem. Commun.*, 129–130.

Beusen, D. D., Carrell, H. L., & Covey, D. F. (1987) *Biochemistry 26*, 7833–7841.

Brodie, A. M. H. (1982) *Cancer Res. 42*, 3312–3314.

Brodie, H. J., Kripalani, K. J., & Possanza, G. (1969) *J. Am. Chem. Soc. 91*, 1241–1242.

Cole, P. A., & Robinson, C. H. (1988) *J. Am. Chem. Soc. 110*, 1284–1285.

Covey, D. F., Hood, W. F., Beusen, D. D., & Carrell, H. L. (1984) *Biochemistry 23*, 5398–5406.

Covey, D. F., Carrell, H. L., & Beusen, D. D. (1987) *Steroids 50*, 363–374.

Dewar, M. J. S., Zoebisch, E. G., Healy, E. F., & Stewart, J. (1985) *J. Am. Chem. Soc. 107*, 3902–3909.

Duax, W., Norton, D., Pokrywiecki, S., & Eger, C. (1971) *Steroids 18*, 525–544.

Engle, L. L. (1973) in *Handbook of Physiology and Endocrinology, Part 1* (Greep, R., Astwood, S., & Geiger, B., Eds.) Vol. 2, pp 467–483, American Physiological Society, Washington, DC.

Fishman, J., Guzuk, H., & Dixon, D. (1969) *Biochemistry 8*, 4304–4309.

Friedrich, B., Herman, Z., Zahradnik, R., & Havlas, Z. (1988) *Adv. Quantum Chem. 19*, 247–288.

Guengerich, F. P. (1987) *Mammalian Cytochromes P-450, Vol. 1 and 2*, CRC Press, Boca Roton, FL.

Kellis, J. T., Jr., Childers, W. E., Robinson, C. H., & Vickery, L. E. (1987) *J. Biol. Chem. 262*, 4421–4426.

Korzekwa, K. R., Trager, W. F., Nagata, K., Parkinson, A., & Gillette, J. R. (1990a) *Drug Metab. Dispos. 18*, 974–979.

Korzekwa, K. R., Jones, J. P., & Gillette, J. R. (1990b) *J. Am. Chem. Soc. 112*, 7042–7046.

Marcotte, P. A., & Robinson, C. H. (1982) *Biochemistry 21*, 2773–2778.

Nagata, K., Liberato, D. J., Gillette, J. R., & Sasame, H. A. (1986) *Drug Metab. Dispos. 14*, 559–565.

Ortiz de Montellano, P. R (1987) *Cytochrome P-450, Structure, Mechanism, and Biochemistry*, Plenum Press, New York.

Ortiz de Montellano, P. R (1989) *Trends Pharmacol. Sci. 10*, 354–359.

Osawa, Y. (1973) in *Endocrinology, Proceedings of the 4th International Congress of Endocrinology* (Scow, R. O., Ed.) pp 814–819, Excerpta Medica, Amsterdam.

Osawa, Y., & Spaeth, D. G. (1971) *Biochemistry 10*, 66–71.

Osawa, Y., Higashitama, T., Fronckowiak, M., Yoshida, N., & Yarborough, C. (1987a) *J. Steroid Biochem. 27*, 781–789.

Osawa, Y., Yoshida, N., Fronckowiak, M., & Kitawaki, J. (1987b) *Steroids 50*, 11–28.

Osawa, Y., Osawa, Y., & Coon, M. J. (1987c) *Endocrinology 121*, 1010–1015.

Osawa, Y., Martin, B. M., Griffin, P. R., Yates, J. R., Shabanowitz, J., Hunt, D. F., Murphy, A. C., Chen, L., Cotter, R. J., & Pohl, L. R. (1990) *J. Biol. Chem. 265*, 10340–10346.

Osawa, Y., Highet, R. J., Bax, A., & Pohl, L. R. (1991) *J. Biol. Chem. 266*, 3208–3214.

Rettie, A. W., Rettenmeier, A. W., Howald, W. N., & Baillie, T. A. (1987) *Science 235*, 890–893.

Rettie, A. W., Boberg, M., Rettenmeier, A. W., & Baillie, T. A. (1988) *J. Biol. Chem. 263*, 13733–13738.

Ryan, K. J. (1959) *J. Biol. Chem. 234*, 268–272.

Santen, R. J. (1882) *Cancer Res. 42*, 3268.

Siiteri, P. K. (1982) *Cancer Res. 42*, 3269–3273.

Stevenson, D. E., Wright, J. N., & Akhtar, M. (1985) *J. Chem. Soc., Chem. Commun.* 1078–1080.

Thompson, E. A., Jr., & Siiteri, P. K. (1974) *J. Biol. Chem. 249*, 5364–5372.

Townsley, J. D., & Brodie, H. J. (1968) *Biochemistry 7*, 33–40.
Van Wauwe, J. P., & Janssen, A. J. (1989) *J. Med. Chem. 32*, 2231–2239.
Watanabe, Y., & Ishimura, Y. (1989a) *J. Am. Chem. Soc. 111*, 410–411.
Watanabe, Y., & Ishimura, Y. (1989b) *J. Am. Chem. Soc. 111*, 8047–8049.

Rotational Mobility of High-Affinity Epidermal Growth Factor Receptors on the Surface of Living A431 Cells†

Raphael Zidovetzki,*,‡ David A. Johnson,§ Donna J. Arndt-Jovin,∥ and Thomas M. Jovin*,∥
Department of Biology and Division of Biomedical Sciences, University of California, Riverside, California 92521, and Abteilung Molekulare Biologie, Max-Planck-Institute für Biophisikalische Chemie, W-3400 Göttingen, FRG
Received January 9, 1991; Revised Manuscript Received March 16, 1991

ABSTRACT: The rotational diffusion of epidermal growth factor (EGF) bound to its specific receptor on the surface of human carcinoma A431 cells was studied by means of time-resolved phosphorescence anisotropy measurements. The rotational mobility was measured on the total population of EGF receptors by using a saturating concentration of EGF conjugated with a phosphorescent label, erythrosin, or on the subpopulation of high-affinity EGF receptors by using a low concentration of labeled EGF. At 4 °C, the rotational correlation times for both the high-affinity and total (mostly low affinity) receptor populations were in the range of 60–100 μs. Elevation of the temperature to 37 °C resulted in a lengthening of the rotational correlation time of the total receptor population to 200–300 μs, confirming a previous study of receptor microaggregation. The high-affinity EGF receptors were completely immobilized at 37 °C (rotational correlation time >500 μs). The data are consistent with a model involving association of the cytoskeleton with the high-affinity receptors at 37 °C, but not at 4 °C.

Epidermal growth factor (EGF)[1] is a 6045-Da polypeptide which binds to specific membrane receptors (EGFR) present as integral membrane proteins in a wide variety of cells (Carpenter & Cohen, 1979; Adamson & Rees, 1981). Binding initiates a number of biochemical processes including activation of intrinsic tyrosine kinase activity (Cohen et al., 1982; Buhrow et al., 1983), increased ion and metabolite transport, and stimulated proliferation of the target cells (Gospodarowicz et al., 1978; Carpenter & Cohen, 1979). EGFR is one of the most studied cell-surface receptors. Its primary amino acid sequence has been deduced by Ullrich et al. (1984), who also provided a tentative identification of an external hormone binding domain, a single membrane-spanning domain, and a cytoplasmic domain which exhibits the tyrosine kinase activity. EGFR is a member of a family of receptors with certain common features in their mechanism of action [see Gill et al. (1987), Carpenter (1987), Yarden and Ullrich (1988), and Schlessinger (1988) for reviews].

Two general mechanisms have been suggested to explain the transmembrane signal transduction by EGFR (Schlessinger, 1986; Basu et al., 1986): (1) EGF binding induces a conformational change of the receptor that propagates through the membrane by a single membrane-spanning domain of EGFR (intramolecular mechanism); (2) EGF binding induces a change in receptor–receptor interaction leading to activation of the cytoplasmic tyrosine kinase (intermolecular mechanism). Both mechanisms have experimental support (Basu et al., 1986; Koland & Cerione, 1988; Yarden & Schlessinger, 1987a,b; Boni-Schnetzler & Pilch, 1987).

The intermolecular mechanism was proposed to involve "microclustering" of EGFR as a necessary prerequisite for the biological response (Schlessinger et al., 1983). Indeed, EGF induces rapid formation of small receptor aggregates (not distinguishable by light microscope) immediately following binding to EGFR (Carpenter & Cohen, 1976; Zidovetzki et al., 1981). Receptor aggregation was recently shown to be linked to a modification of the tyrosine kinase activity of EGFR (Carraway et al., 1989). Formation of microclusters of EGFR upon EGF binding was also demonstrated on cell-free A431 cell membrane suspensions (Zidovetzki et al., 1986; Azevedo & Johnson, 1991). Moreover, EGF-induced dimerization of EGFR has been observed with detergent-solubilized preparations of EGFR (Boni-Schentzler & Pilch, 1987; Yarden & Schlessinger, 1987a,b; Cochet et al., 1988).

A transition from a mobile to an aggregated state of a receptor takes place in other systems. For example, receptor immobilization was reported after binding of nerve growth factor to its cell-surface receptor (Levi et al., 1980). In the case of insulin, the biological effects of the hormone were mimicked by cross-linking the insulin receptor with specific anti-receptor antibodies [Kahn et al., 1978; Jacobs et al., 1978; see Gill et al. (1987) for a critique of the clustering hypothesis].

The change in mobility, however, does not have to involve receptor self-aggregation; association with other plasma membrane molecules or cytoskeleton would also result in reduced receptor mobility. In the latter case, complete immobilization of the receptors would be expected, which would

† This work was supported by Grant BC-590 from the American Cancer Society (to R.Z.).
‡ Department of Biology, University of California.
§ Division of Biomedical Sciences, University of California.
∥ Max-Planck-Institute für Biophisikalische Chemie.

[1] Abbreviations: EGF, epidermal growth factor; Er-EGF, EGF labeled with erythrosin 5′-isothiocyanate; [^{125}I]EGF, EGF labeled with ^{125}I; EGFR, EGF receptor(s); HA-EGFR, high-affinity EGFR; LA-EGFR, low-affinity EGFR; PBS, phosphate-buffered saline.

0006-2960/91/0430-6162$02.50/0